

Characteristic fast-energy losses in rare-earth metals

A. G. Nargizyan and Yu. A. Uspenskii

Lebedev Physics Institute, Russian Academy of Sciences

(Submitted 25 September 1992)

Zh. Eksp. Teor. Fiz. **103**, 1078–1086 (March 1993)

We examine the nature of the singularities in the characteristic energy losses (CEL) of fast electrons in rare-earth metals. A numerical calculation of the CEL function for the entire series of 4*f* metals leads to satisfactory qualitative and quantitative agreement with experiment. The calculations were made within the framework of the density-functional method. It is shown that the main features of the CEL spectrum in rare-earth metals are governed by interband transitions of electrons from the 4*f* to the 5*d* and 6*d* bands, as well as to excitation of 5*p* electrons of the core to higher bands.

1. INTRODUCTION

The unusual physical properties of rare earth metals (REM) are closely related to the partially filled 4*f* shell they contain. The proximity of the energy of the 4*f*-electrons to the Fermi level notwithstanding, they have practically the same spatial localization as the electrons of the closest core levels. The 4*f* electrons exert therefore a very small influence on the interatomic bonds, but make the main contribution to the electronic heat capacity and to the magnetic properties of the REM. In low-energy spectral investigations (ultraviolet photoemission spectroscopy) the excitations of the 4*f* electrons are quite weakly manifest, whereas at high photon energies (x-ray photoemission spectroscopy) they are well pronounced. An important circumstance pointing to a major role of electron correlations is that in x-ray photoemission spectra the maxima corresponding to 4*f* electrons lie not near the Fermi level, as they should in accord with the band theory, but several eV lower. However, the role of 4*f* electrons in optical spectra in the characteristic energy loss (CEL) spectra is still unclear. The experimental dependences of the optical conductivity $\sigma(\omega) = (\omega/4\pi)\text{Im}\epsilon(\omega)$ and the CEL function $L(\omega) = \text{Im}[-1/\epsilon(\omega)]$ show no singularities whatever attributable unambiguously to 4*f*-electron excitations.^{1–3} To a certain degree, a possible explanation is that strongly localized 4*f* orbitals overlap weakly the wave functions of other valence electrons, so that the matrix elements of the transition between these states are small. However, the large number of 4*f*-electrons per REM atoms attests to their large contribution to the *f*-sum rule and to the appreciable oscillator strength of the corresponding transitions. Another unanswered question, likewise connected with 4*f*-electrons, is the influence of electron correlations on the formation of the optical characteristics and spectra of the CEL.

Elucidation of these topics can be substantially facilitated by microscopic calculations of the optical and CEL spectra. As a rule, such calculations are made in the framework of a band approach based on the self-consistent Kohn–Shem equations.⁴ Experience shows that the spectra calculated in this manner for simple, noble, and *d*-transition metals agree well with the experimental data and make it possible to explain their most salient features.^{5,6} As already noted above, microscopic calculations for REM are hindered by strong intra-atomic correlations due to localization of the 4*f* elec-

trons. The correlations are usually described by the Hubbard or by the Anderson model. The complexity of these models, however, makes it necessary to simplify greatly the description of the electron structure, and to compensate for this choose model parameters that lead to best agreement with experiment. This decreases substantially the possibility of using model calculations for the interpretation of REM spectra. We have therefore preferred to use a microscopic calculation of $\sigma(\omega)$ and $L(\omega)$ in the framework of the band approach, where no fit parameters are needed, and confining ourselves to that description of multielectron correlations which corresponds to the local-density approximation. The results are used to determine the main group of electron transitions that form the CEL and REM spectrum, to cast light on the role of the 4*f*-electrons, and to analyze the tendencies of the variation of the spectral characteristics along the 4*f* series.

2. MICROSCOPIC CALCULATION

Our task was to calculate the CEL spectra of all the rare-earth metals from Ce to Lu for energy transfers $\hbar\omega \leq 45$ eV. The corresponding experimental data were published in Ref. 3. The only exceptions were the metals Pm and Sm, which have complicated crystal structures not considered in this study.

Microscopic calculations in the spectral region of interest require, beside excitations of valence 6*s*-, 6*p*-, 5*d*-, and 4*f*-electrons, to take into account also excitations of the core 5*s* and 5*p* levels approximately 45 and 20 eV lower than the Fermi level. Another important factor influencing the spectral characteristics is the exchange splitting of the 4*f* band, which reaches about 7 eV in Eu and Gd. The exchange splitting in the 5*d* band is significantly weaker—about 1 eV. The above numerical values pertain to the ferromagnetic state, which is realized in the metals Dy, Gd, and Tb. In Eu, however, the spin ordering is antiferromagnetic, while in Ho, Er, Tm, Pr, and Nd even more complicated spin structures are formed. It must be noted that the orientation differences of spins belonging to different angles of the crystal lattice influences only the electrons of the 6*s*, 6*p*, and 5*d* bands, and also the internal structure of each of the exchange-split halves of the 4*f* band, i.e., it has an energy scale smaller than 1 eV. On the other hand the exchange splitting of the 4*f*

band, determined mainly by the intra-atomic parameters, remains unchanged here. Since the CEL spectra are insensitive to changes of the electron structure over a scale $\Delta E \leq 1$ eV, all our calculations were carried out only for the ferromagnetic state and required substantial computation time.

A few more details concerning the calculation itself. A self-consistent computation of the electron structure was carried out by the LMTO (linear muffing-tin orbitals) method⁷ with combined corrections taken into account. We used a scalar-relativistic approximation, and the exchange-correlation potentials were chosen as in Ref. 8. The number of k -points in the irreducible part of the Brillouin zone was taken to be 55 for BCC metals (Eu), 88 for FCC metals (Ce, Yb), and 75 for metals with ordinary (Gd, Dy, Tb, Ho, Er, Tm, Lu) and double (Pr, Nd) FCP structures. The calculations were performed using experimental lattice parameters. An indirect feature of the quality of the obtained self-consistent potential may be the fact that the equilibrium lattice parameter calculated with their aid differed from the experimental ones by not more than 1%. Note also that our electron dispersion curves $E_\lambda(k)$ agree well with the calculation data of Refs. 9 and 10.

The permittivity tensor was calculated in the random-phase approximation with allowance for local-field effects:

$$\varepsilon_{\alpha\beta}(\omega) = \delta_{\alpha\beta} - \frac{\tilde{\omega}_{p\alpha\beta}^2}{\omega(\omega + i\delta)} - \frac{8\pi\hbar e^2}{\Omega m^2} \sum_{\mathbf{k}, n \neq n'} \frac{f_{\mathbf{k}, n} - f_{\mathbf{k}, n'}}{(E_{\mathbf{k}, n} - E_{\mathbf{k}, n'})^2 (\hbar\omega - E_{\mathbf{k}, n'} + E_{\mathbf{k}, n} + i\delta)} \times \langle \mathbf{k}, n | p_\alpha | \mathbf{k}, n' \rangle \langle \mathbf{k}, n' | p_\beta | \mathbf{k}, n \rangle, \quad (1)$$

where Ω is the unit-cell volume, \mathbf{k} and n are the wave vector in the first Brillouin zone and the number of the electron-spectrum branch, \mathbf{p} is the momentum operator, and the intraband plasma frequency ω_p is determined by the electronic transitions near the Fermi surface:

$$\hbar^2 \tilde{\omega}_{p\alpha\beta}^2 = \frac{4\pi e^3 m}{3\Omega} \sum_{\mathbf{k}, n} (\nabla_{\mathbf{k}\alpha} E_{\mathbf{k}n}) (\nabla_{\mathbf{k}\beta} E_{\mathbf{k}n}) \delta(E_{\mathbf{k}, n} - E_F). \quad (2)$$

The first term in (1) corresponds to the contribution, described using the Drude equation, of the intraband transitions, and the second corresponds to transitions from a band numbered n to one numbered n' . Since the energy interval $\hbar\omega$ is large enough, the electron structure must be described using the LMTO method with three panels: the lower for the core $5s$ and $5p$ states, the middle one for the valence $6s$, $6p$, $5d$, and $4f$ states, and the upper for the high-energy band of the conduction band, made up of strongly hybridized $6d$, $5f$, $5g$ orbitals. In the lower panel we took into account the spin-orbit splitting of the $5p$ -level, approximately 4 eV, whereas the spin-orbit splitting of the $4f$ -valence states, equal to 0.8 eV for Eu, was not taken into account in our calculation. Note also that to calculate $\varepsilon_{\alpha\beta}(\omega)$ we used approximately 2.5 times more \mathbf{k} points than were used Refs. 5, 11, and 12, where the treatment was more detailed.

3. CEL SPECTRA AND OPTICAL CONDUCTIVITIES OF RARE-EARTH METALS

The calculated spectra of the energy losses of REM fast electrons are shown in Fig. 1, together with experimental

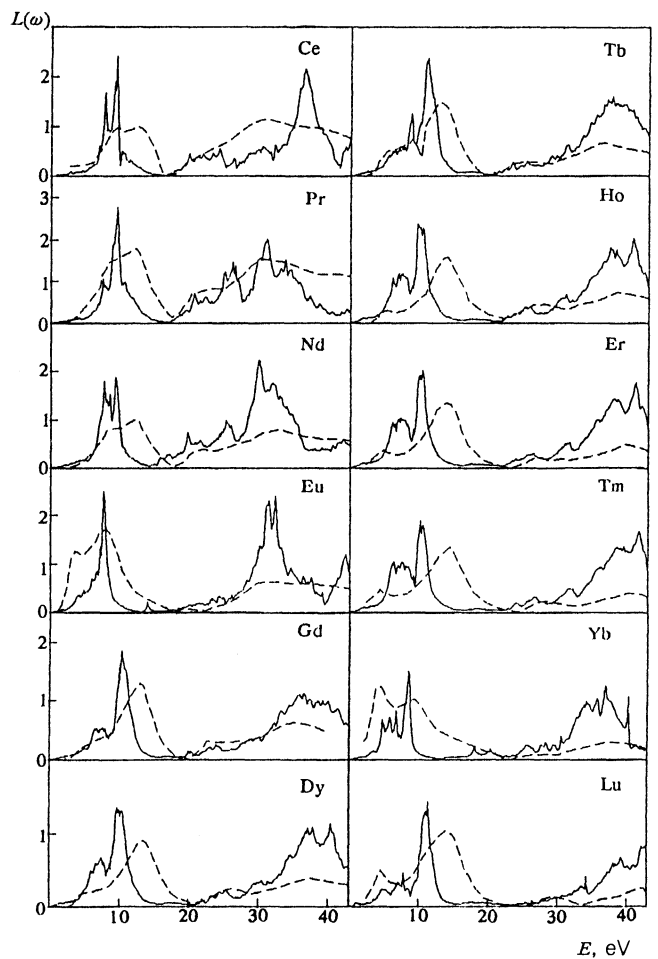


FIG. 1. CEL function $L(\omega)$ in REM: solid line—calculation, dashed—experiment.³

data taken from Ref. 3. The CEL spectra of all the rare-earth metals are strikingly similar. They have a split low-frequency maximum with energy close to 10 eV and a broad maximum at 35 eV. Along the $4f$ series from Ce to Lu the position of the low-frequency maximum remains practically unchanged, except for Eu and Lu, whereas the high-frequency maximum increases gradually from 30 eV in Ce to 42 eV in Lu. All these qualitative features of the CEL spectra of rare-earth element are in splendid agreement with the numerical calculation. To be sure, calculations undervalue somewhat the position of the low-frequency maximum (by 2 eV on the average), and the intermediate maximum with approximate energy 25 eV, well distinguishable on the experimental curves of heavy REM, is somewhat weaker on the calculated plots. In addition, the amplitudes of the high-energy maximum is larger in the calculation than in the experiment. These differences can be caused, to a considerable degree, by the fact that the calculations were made for a momentum transfer $\mathbf{q} = 0$, which is realized in experiments on the passage of fast electrons through metal films. Actually, in measurements¹³ by such a procedure, there is no maximum with energy close to 25 eV, and the amplitudes of the high-energy and low-frequency maxima are almost equal. The experimental data³ of Figs. 1 and 2, however, were obtained for reflection of fast electrons from the sample surface, i.e., were

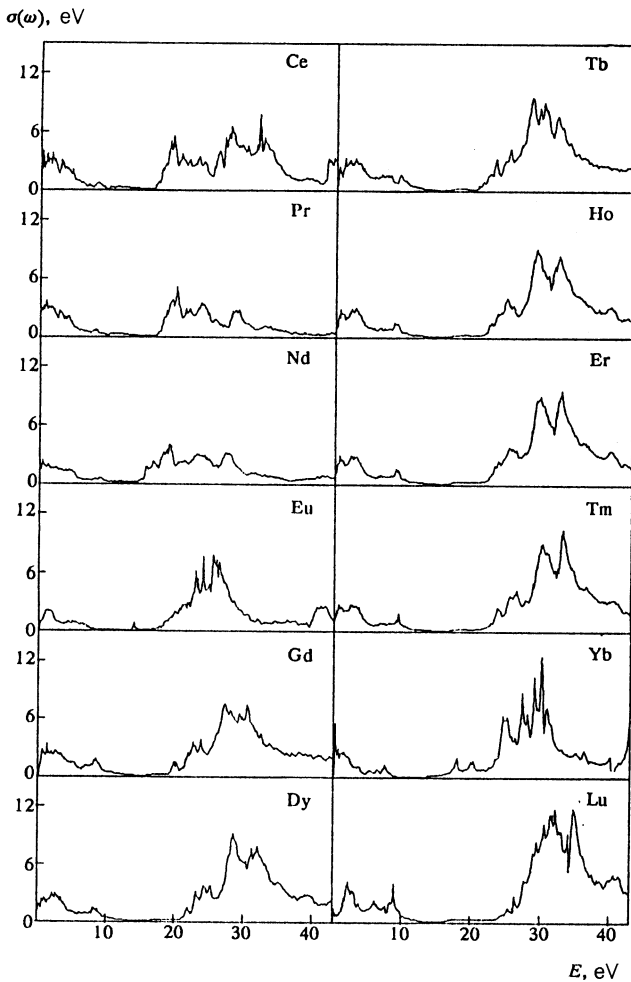


FIG. 2. Interband optical conductivity in REM.

averages over the momentum transfer and could in part include also surface plasmons.

Let us determine now which electronic excitations participate in the formation of the characteristic-loss spectrum. Figure 2 shows calculated plots of the optical interband conductivity of all the considered REM. Figure 3 shows, with Eu as the example, which group of transitions forms the optical conductivity in 4f metals. It can be seen that in all the rare-earth metals the optical conductivity has two large maxima. The first, corresponding to an energy $\hbar\omega < 10$ eV, is produced by intraband transitions with energies $\hbar\omega \leq 0.5$ eV (not shown in Fig. 2), by interband transitions inside the 5d band, and by transitions from the 4f to the 5f band or, on the contrary, from 5d into 4f. The last two groups of transitions, connected with the presence of a 4f band, have an approximate oscillator strength 1.5 electron/atom. The oscillator strength of the entire low-frequency maximum is about 3.0 electrons/atom, i.e., approximately equal to the typical chemical valency of the rare-earth metals. This agreement seems natural at first glance. If it is recalled, however, that chemical valency is connected with the proportions of the components in a molecule or a chemical compound, this equality ceases to be so obvious. After all, 4f electrons, which play a very small part in the formation of the interatomic band, contribute almost 50% to the f-sums at $\hbar\omega < 10$ eV.

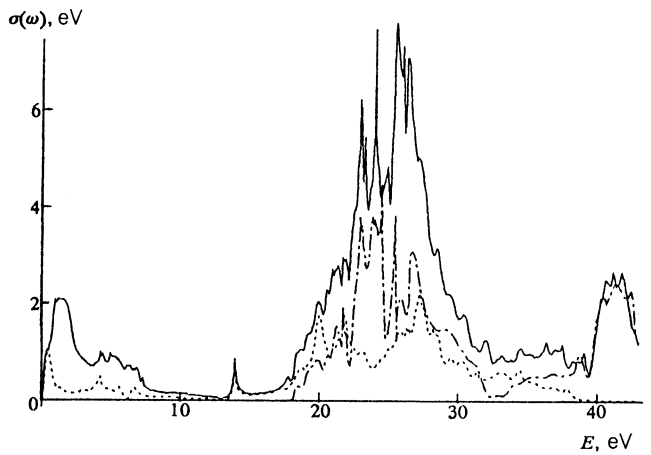


FIG. 3. Interband optical conductivity in europium: solid line—total conductivity, dashed—contribution of 4f-band, dotted—contribution from excitation of the skeleton 5p electrons.

The second maximum of the optical conductivity has an energy 20–35 eV. It is formed mainly by interband 4f–6d transitions and excitations of 5p-electrons of the core. Note that the strength of the oscillators of 4f–6d transitions of 4–6 electrons/atom, i.e., more than triple the contribution of the 4f band in the low-frequency region. Since, however, the energies of the 4f–6d transitions and of the excitations of the 5p-electrons of the core are almost equal, it is practically impossible to separate from the total curve the contribution of the 4f-electrons.

The presence of two optical-conductivity electrons greatly separated in energy leads to the characteristic two-peak form of the CEL spectrum. The mechanism of its formation is similar in many respects to that proposed in Ref. 6 to explain the complicated spectrum of plasmons in 4d-transition metals. Let us illustrate this using as an example the optical-conductivity model

$$\sigma(\omega) = \frac{1}{8} \Omega_p^2 [N_1 \delta(\omega) + N_2 \delta(\omega - \omega_2)]. \quad (3)$$

Here $\Omega_p = (4\pi e^2/m\Omega)^{1/2}$ is the classical plasma frequency corresponding to a density of one electron per atom, N_1 and N_2 are the oscillator strengths of the low- and high-energy transition groups. The corresponding characteristic-loss function is

$$L(\omega) = \frac{\pi \Omega_p^2}{2} \left[\frac{\tilde{N}_1}{\omega_{p1}} \delta(\omega - \omega_{p1}) + \frac{\tilde{N}_2}{\omega_{p2}} \delta(\omega - \omega_{p2}) \right]. \quad (4)$$

Here the plasma frequencies ω_{p1} and ω_{p2} are determined by the positions of the zeroth of the permittivity. These frequencies, as well as the effective electron numbers \tilde{N}_1 and \tilde{N}_2 are given by

$$\omega_{p1,2} = \Omega_p \left\{ \frac{1}{2} \left(\frac{\omega_2}{\Omega_p} + N_1 + N_2 \right) \mp \left[\frac{1}{4} \left(\frac{\omega_2}{\Omega_p} + N_1 + N_2 \right)^2 - N_1 \frac{\omega_2}{\Omega_p} \right]^{1/2} \right\}^{1/2},$$

$$\tilde{N}_1 + \tilde{N}_2 = N_1 + N_2, \quad (5)$$

$$\tilde{N}_1 = \frac{\omega_{p1}^2 (\omega_2^2 - \omega_{p1}^2)}{\Omega_p^2 (\omega_2^2 - \omega_{p1}^2)}$$

In the case of 4*d*-transition metals the values of the parameters are such that $\Omega_p N_1^{1/2} > \omega_2$. As a result the frequency of a low-energy plasmon presses so to speak towards the frequency ω_2 , so that $\omega_{p1} \ll \omega_2$. In 4*f* transition metals the situation is more readily the opposite. Here $\Omega_p N_1^{1/2} \ll \omega_2$, so that $\omega_{p1} \approx \Omega_p (N_1/\epsilon_0)^{1/2}$, where ϵ_0 is the static permittivity due to electron transitions of energy $\hbar\omega_2$. For Eu we have $\hbar\Omega_p = 5.3$ eV, $N_1 = 2.8$, $\epsilon_0 = 1.7$, so that $\hbar\omega_{p1} = 6.8$ eV, in good agreement with experiment. Since the static dielectric constant ϵ_0 is close to 1 while $N_1 \approx 3$, the energy $\hbar\omega_{p1}$ turns out to be close to the classical plasma energy calculated for three electrons per atom: $\hbar\omega_p (N = 3) = 9.2$ eV. Similar results are obtained also for other rare-earth elements. They explain the empirical fact¹⁴ that the low-energy plasmon energy is quite close to that of a low-temperature plasma of energy $\hbar\omega (N = 3)$.

As to the second maximum of the CEL function $L(\omega)$, to which corresponds in the model (3) a delta-shaped peak with energy $\hbar\omega_{p2}$, its width in real metals turns out to be quite large—on the order of 5–7 eV. Its location, width, and shape are determined mainly by the location of the 6*d*-band and the 5*p*-core states relative to the Fermi level E_F . At the start of the 4*f* series (Ce, Pr) the energy $E_{6d} - E_F$ is almost 10 eV higher than $E_F - E_{5p}$. On going to the end of the 4*f* series, the energy difference $E_{6d} - E_F$ changes relatively little, whereas the depth of the location of the frame 5*p* level grows almost to 8 eV owing to the increase of the charge of the nucleus. The result is a noticeable increase of the energy of the high-frequency maximum of the function $L(\omega)$, accompanied by a definite change of its form.

4. CONCLUSION

The foregoing calculations show that the 4*f* electrons make a substantial contribution to the *f*-sum rule, especially

at energies $\hbar\omega \leq 10$ eV. This contribution determines to a considerable degree the position of the low-energy plasmon present in the CEL spectra of all rare-earth metals. In the high-frequency region, however, where the 4*f* electrons make the largest contribution because of the strong localization, their excitation energies almost coincide with the excitation region of the skeleton 5*p* electrons, so that it is practically impossible to separate the contribution of the 4*f* electrons in pure form. No specific maximum that might be due entirely to 4*f* electrons could be observed in the CEL spectra. As to the role of electron correlations, the data show that in optics and in CEL spectra their values are not very significant—on the order of 2 eV or less. More detailed information on this can be probably obtained by analyzing the optical and magneto-optical spectra at energies on the order of several electron volts.

The authors thank K. A. Kikoin for helpful discussion and to S. N. Rashkevich for help with the work.

¹Yu. V. Knyazev and M. M. Noskov, Phys. Stat. Sol. (b) **80**, 11 (1977).

²J. H. Weaver and D. W. Lynch, Phys. Rev. B **7**, 4737 (1973).

³F. P. Netzer, G. Strasser, G. Rosina, and J. A. D. Matthew, Surf. Sci. **152/153**, 757 (1985).

⁴Theory of inhomogeneous electron gas, S. Lundquist and S. March, eds. [Russ. transl.], Mir, Moscow (1987).

⁵E. G. Maksimov, I. I. Mazin, S. N. Rashkeev, and Yu. A. Uspenskiĭ, J. Phys. F **18**, 833 (1988).

⁶I. I. Mazin, E. G. Maksimov, S. N. Rashkeev, and Yu. A. Uspenskiĭ, Zh. Eksp. Teor. Fiz. **90**, 1092 (1986) [Sov. Phys. JETP **63**, 637 (1986)].

⁷O. K. Andersen, Phys. Rev. B **12**, 3060 (1975).

⁸U. Von Barth and L. Hedin, Solid State Phys. **4**, 2064 (1971).

⁹B. I. Min, H. J. F. Jansen, T. Oguchi, and A. J. Freeman, J. Magn. Magn. Mat. **59**, 277 (1986).

¹⁰W. E. Pickett, A. J. Freeman, and D. D. Koelling, Phys. Rev. B **22**, 2695 (1980).

¹¹Yu. A. Uspenskiĭ, E. G. Maksimov, S. N. Rashkeev, and I. I. Mazin, Z. Phys. B **53**, 263 (1983).

¹²A. G. Nargizyan, S. N. Rashkeev, and Yu. A. Uspenskiĭ, Fiz. Tverd. Tela **34**, 1042 (1992) [Sov. Phys. Solid State **34**, (1992)].

¹³C. Colliex, M. Gasgnier, and P. Trebbia, J. Phys. **37**, 397 (1976).

¹⁴F. P. Netzer and J. A. D. Matthew, *Handbook of Physics and Chemistry of Rare Earth*, K. A. Gschneider, L. Eyring, and S. Hufner, eds. Vol. 10, Elsevier, (1987), p. 547.

Translated by J. G. Adashko